AIAA JOURNAL
Vol. 38, No. 9, September 2000

Improved Electrorheological-Fluid Variable Damper Designed for Semiactive Vibration Suppression

Junjiro Onoda,* Hyun-Ung Oh,† and Kenji Minesugi‡
Institute of Space and Astronautical Science, Sagamihara, Kanagawa 229-8510, Japan

The studied damper can be modeled as a variable coulomb-friction damper. The friction in the damper is not zero, even when no voltage is applied to the electrode of the damper, and is an increasing function of the absolute value of the voltage. Semiactive vibration suppression exploits this variation of friction. To suppress large-amplitude vibrations to small-amplitude ones effectively, we need to vary the friction over a large range. In other words, the ratio of the maximum and minimum values of the frictional force needs to be large. An investigation of decreasing the minimum frictional force by vibrating the electrode of the damper to increase this ratio is reported. The effectiveness of the electrode vibration was demonstrated in static experiments, as well as in semiactive vibration suppression experiments, indicating that electrode vibration reduces the minimum frictional force by $\frac{1}{3}$–$\frac{1}{2}$ without changing the maximum frictional force, thereby greatly reducing the vibration amplitude.

Nomenclature

c = viscous coefficient of the viscous element of the damper model (Fig. 2)
d = elongation of the damper
e = elongation between points 2 and 4 of the damper model (Fig. 2)
e_T = target value of e given by Eq. (14) of Ref. 6
F_1, F_2 = elements of the gain matrix given by the linear quadratic regulator control theory as described in Ref. 6
f = maximum frictional force of the coulomb-frictional element of the damper model (Fig. 2)
g = tensile load at point 3 of the damper model (Fig. 2)
h_1, h_2 = fluid levels in cylinders 1 and 2
k_1, k_2 = spring constants of the springs of the damper model (Fig. 2)
p = tensile load on the damper
u_1, u_2 = lateral displacements of the tip mass and a central node of a truss (Fig. 11)
V = input voltage applied to the electrode of the damper

Subscripts

max, min = maximum and minimum values

Introduction

SEMIACTIVE vibration suppression controls the states of systems in such a way that their inherent vibration damping is enhanced.[1–5] Because vibration is, thus, suppressed by exploiting passive energy dissipation mechanisms (structural damping, viscosity, friction, etc.), structures are stable even when the control logic is improper as a result of the lack of exact information about their dynamic characteristics. This robustness is a great advantage of the semiactive approach over active vibration suppression. Although structural systems used in outer space are required to be extremely reliable, the dynamic characteristics of structures that are deployed or constructed in orbit are very difficult to predict accurately. The robust semiactive approach to vibration suppression is, therefore, especially suitable for space structures.

To implement semiactive vibration suppression, Onoda et al.[6] made a variable damper consisting of two variable-volume chambers filled with an electrorheological (ER) fluid connected by a bottleneck with an electrode in it (Fig. 1). The characteristics of the ER fluid between the electrode and the casing of the bottleneck vary according to the voltage applied to the electrode, thus varying the characteristics of the damper. Based on the measured characteristics of a damper filled with an ER fluid consisting of carbonaceous particles in silicone oil, they modeled the damper as shown in Fig. 2. The model is composed of two springs, a viscous element, and a variable coulomb-frictional element. When a high voltage is applied to the electrode, the flow friction in the bottleneck increases, thus increasing f of the frictional element of the damper model shown in Fig. 2. They also showed by numerical simulations and experiments that the vibrations of truss structures could be nicely suppressed by controlling the variable damper and that the performance of this semiactive vibration suppression was better than that of the optimal passive vibration suppression.

In the experiments reported on in Ref. 6, semiactive vibration suppression was effective when the vibration amplitude was large but was almost useless when the vibration amplitude had been reduced to a small level. The reason for this degradation of vibration suppression performance was because the vibration had been suppressed to so small an amplitude that the load on the frictional element of the damper model in Fig. 2 did not exceed even the minimum value of f, that is, $f_{\min}$ (which is the value of f when the input voltage is zero), and the frictional element stuck. Onoda et al. also showed that the value of $f_{\min}$ measured just after turning off the voltage to the electrode was substantially larger than the value measured when no voltage was applied. They pointed out that $f_{\min}$ needed to be reduced if the vibration were to be reduced further.

The value of $f_{\min}$ can easily be reduced by changing the dimensions of the damper, for example, shortening the bottleneck or increasing its diameter. However, because this would also reduce $f_{\max}$ (the value of f when the maximum input voltage is applied), the damper would no longer suppress large-amplitude vibrations well. Therefore, we need to reduce $f_{\min}$ without reducing $f_{\max}$, or increase $f_{\max}/f_{\min}$.

This paper shows how the value of $f_{\min}$ can be reduced without reducing $f_{\max}$, that is, the performance of the ER-fluid variable damper can be improved, by vibrating the electrode at a high frequency using a piezoelectric vibrator.

Modification of the ER-Fluid Damper

Because the ER-fluid damper shown in Fig. 1 has no slip faces of solid parts, the frictional force of the damper mainly originates from

Presented as Paper 98-1920 at the AIAA/ASME/ASCE/AHS/ASC 39th Structures, Structural Dynamics, and Materials Conference, Long Beach, CA, 20–23 April 1998; received 16 August 1999; revision received 16 December 1999; accepted for publication 21 December 1999.

*Professor, Research Division for Space Transportation, 3-1-1 Yoshinodai. Associate Fellow AIAA.
†Postdoctoral Researcher, Research Division for Space Transportation, 3-1-1 Yoshinodai.
‡Associate Professor, Research Division for Space Transportation, 3-1-1 Yoshinodai. Member AIAA.

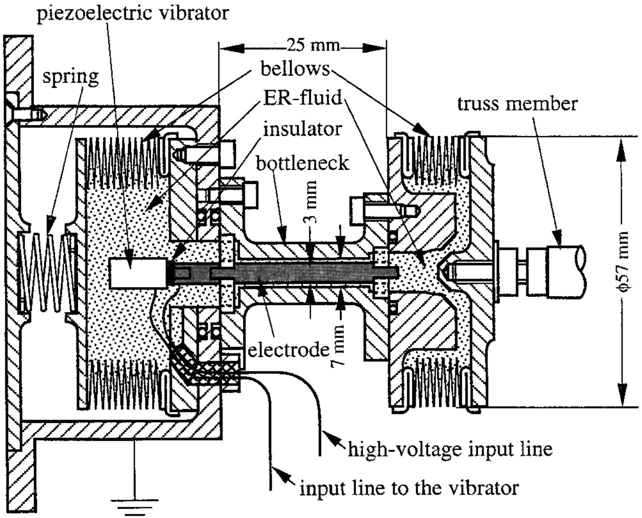

Fig. 1 Cross section of ER-fluid variable damper,[6] with newly attached piezoelectric vibrator.

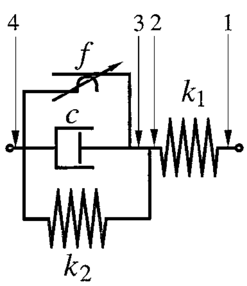

Fig. 2 Model of the ER-fluid damper shown in Fig. 1.

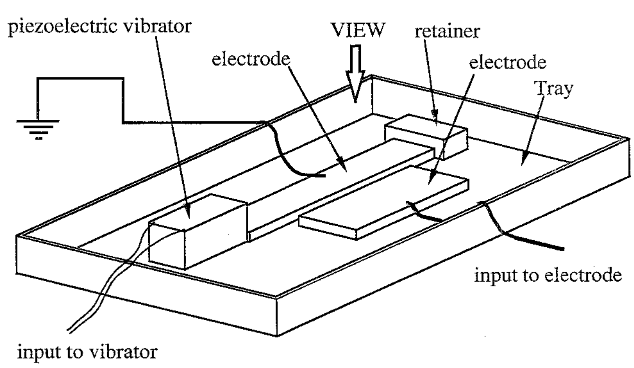

Fig. 3 Experiment setup for microscopic observation of ER-fluid behavior.

the flow friction in the bottleneck. A possible reason for the relatively large value of f_{min} measured just after turning off the high voltage may be an increased flow friction due to ER-fluid microstructure remaining around the electrode even after the high voltage is turned off. To explore the possibility of a high-frequency vibration of the electrode to destroy such a microstructure, we first observed the microstructure of an ER fluid subjected to an electric field. The ER fluid used in the work reported here was Bridgestone NS-6, the same fluid used in the work reported on in Ref. 6.

As shown in Fig. 3, two electrode plates were placed in a shallow ER fluid in a transparent tray 2 mm apart from each other, and a piezoelectric vibrator was attached to one of them. The microstructure of the fluid between the electrodes was observed by using an optical microscope. The ER fluid in the tray was diluted so that the light from the backside of the tray penetrated it. Figure 4a shows the state of the fluid before the electric field was applied. Micrometer-sized particles were dispersed in it. When a 3-kV voltage was applied to one of the electrodes, the particles formed chains just like those shown in Fig. 4b. Then the 3-kV voltage was turned off, and the behavior of the particle chain was observed with and without the electrode vibration. When the electrode was not vibrated, the chains

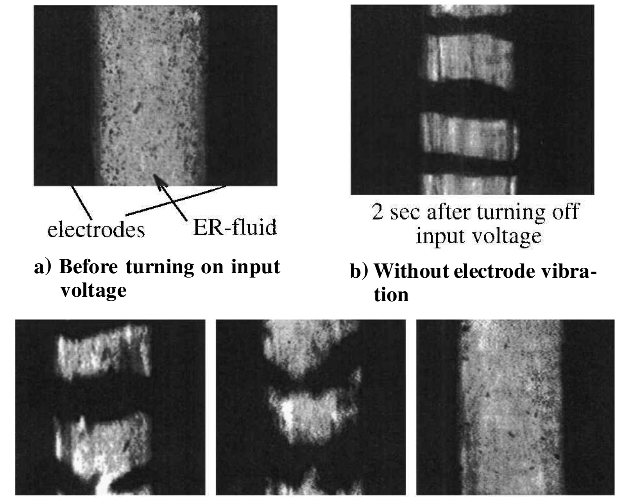

a) Before turning on input voltage

b) Without electrode vibration

c) With electrode vibration 0.3 s, 0.47 s, and 0.7 s after turning off input voltage

Fig. 4 Behavior of ER fluid with and without an electric field.

of particles persisted, as shown in Fig. 4b, even for 2 s after the high voltage to the electrode was turned off. However, when a 1.7-kHz vibration of one of the electrodes was excited at the moment the high voltage to the electrode was turned off, the chains of particles were destroyed quickly, as shown in Fig. 4c. The amplitude of the electrode vibration was approximately 600 m/s^2 at the retainer-side end of the electrode. This suggested that high-frequency vibration of the electrode can quickly destroy the microstructure.

Therefore, we attached a tiny piezoelectric vibrator to the electrode of the variable damper as shown in Fig. 1 and excited a high-frequency axial vibration of the electrode expecting that f_{min} would be reduced. The piezoelectric vibrator used in this investigation was a TOKIN NLA-5 × 5 × 18, whose dimensional size was 5 × 5 × 18 mm. Because the input voltage limit of the piezoelectric vibrator was 100 V, we applied to it a sinusoidal voltage whose maximum and minimum values were 100 and 0 V, respectively. In the following experiment, the frequency of the electrode excitation was 1.7 kHz, which was a resonant frequency of the vibrator and the electrode of the damper. The effect of electrode vibration was most significant at that frequency in the frequency range less than 2 kHz. In all of the following experiments except the extension/contraction tests, the electrode vibration was excited only when the input voltage to the electrode was zero so that f_{max} would not be affected by the electrode vibration.

Effect of Electrode Vibration on Flow Friction in the Bottleneck

Because the flow friction in the bottleneck seems to dominate the frictional force of the damper, the effect of the electrode vibration on the flow friction was investigated by using the experimental setup shown in Fig. 5. Two vertical cylinders (cylinders 1 and 2) were connected through the bottleneck of the ER-fluid damper. Cylinder 1 was also connected to a fluid-level adjuster consisting of a vertical cylinder with a piston that could be raised and lowered by turning a screw. The two cylinders, bottleneck of the damper, and the fluid-level adjuster were partially filled with the ER fluid. A noncontact acoustic fluid-level sensor was installed on top of each of cylinders 1 and 2.

We first applied a 3-kV voltage to the bottleneck electrode (basically shutting down the flow in the bottleneck) and then varied the level of the ER fluid in cylinder 1 by using the fluid-level adjuster. Then we turned off the 3-kV input to the electrode and monitored the levels of the ER fluid in the two cylinders to measure the flow friction in the bottleneck just after the turning off the high-voltage input to the electrode.

Some time histories of the difference between the fluid levels in cylinders 1 and 2, $h_1 - h_2$, are shown in Fig. 6. The time histories obtained without electrode vibration show that the levels did not vary, that is, there was no flow in the bottleneck, whenever the

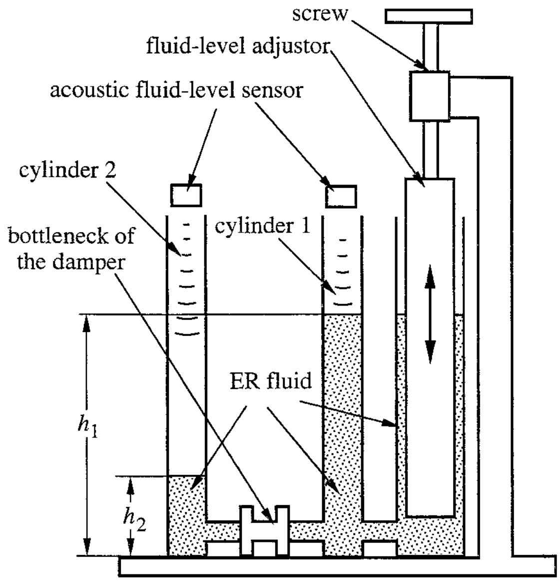

Fig. 5 Experiment setup for measurement of flow friction in the bottleneck.

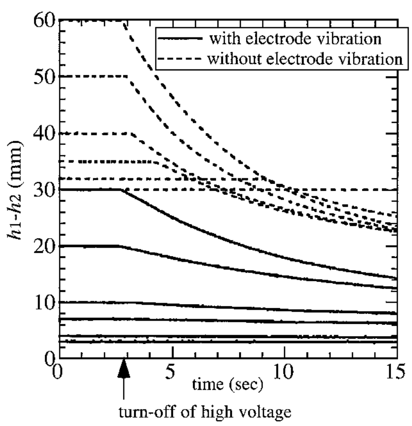

Fig. 6 Time histories of level differences after turning off high-voltage input.

initial level difference, or head, was no more than 30 mm. When the initial head was larger than 35 mm, the variations of the levels started immediately at the moment the input voltage was turned off. When the initial head was 35 mm, the flow started 1.3 s after turning off the input voltage. Because the density of the ER fluid was 1.07 g/cm^3 and the diameter of the bellows of the damper was 57 mm, this suggested that $f_{\min}$ of the damper would be 0.9–1.1 N just after the 3-kV input was turned off. This range includes the value of $f_{\min}$ (1 N) suggested by the semiactive vibration suppression experiment reported in Ref. 6.

When a 1.7-kHz voltage to the electrode vibrator was turned on at the moment the input voltage to the electrode was turned off, the level differences changed, as shown by the solid lines in Fig. 6. They indicated that the flow in the bottleneck started just after the input voltage was turned off even when the initial head was only 30 mm. Precise analysis of the response indicated that the flow in the bottleneck started at the moment the 3-kV input was turned off even when the head was as small as 4 mm, although this is not clear in Fig. 6 because the variation rate of the head was very slow. This indicated that the flow friction in the bottleneck (and thus the value of $f_{\min}$) measured just after the input voltage is turned off can be reduced by vibrating the electrode at a high frequency.

Extension/Contraction Tests of a Damper

As mentioned, the vibration of the electrode should be excited only when the input voltage to the electrode is zero in the semiactive vibration suppression. Therefore, the effect of the electrode vibration on the characteristics of the damper under a nonzero input voltage is not important for vibration suppression. However, for general information, the effect of the electrode vibration on the characteristics of the ER fluid (and, thus, of the damper) was measured in constant-rate extension/contraction tests with and without the input voltage to the electrode.

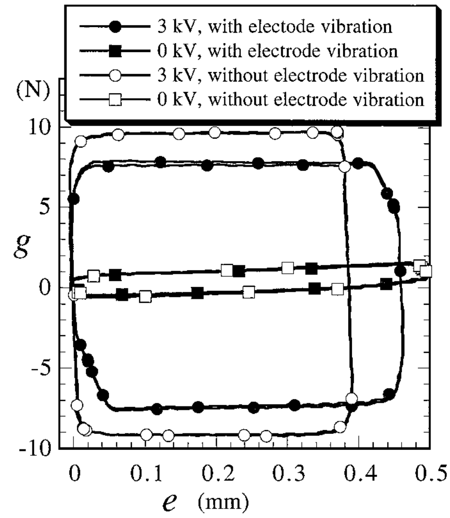

Fig. 7 Load-extension relations measured in extension/contraction tests with and without electrode vibration; extension/contraction rate = 20 mm/min.

Because the viscous element and the coulomb-frictional element of the damper model represent the ER fluid, e–g relations illustrate the characteristics of the ER fluid in the damper more clearly than d–p (extension–load) relations do. Therefore, e–g relations were derived from the measured d–p relations by using the following equations:

$$e = d - p/k_1 \tag{1}$$

$$g = p - k_2 e \tag{2}$$

The values of k_1 and k_2 were estimated from the slopes of the edges of the quadrilateral plots of d–p relations as described in Ref. 6. Figure 7 shows some examples of the thus obtained e–g relations. Note that $\dot{e}$ may not be constant even though $\dot{d}$ is constant during the extension/contraction. Figure 7 shows that the effect of the electrode vibration on the characteristics of the ER fluid was negligible when the input voltage was kept zero although the effect on the flow friction was large as indicated in Fig. 6 just after the input voltage was turned off. This suggests that the electrode vibration reduced the relatively large value of $f_{\min}$ measured just after the input voltage to the electrode was turned off to the value measured without applying the input voltage by destroying the chains of particles in the ER fluid. However, when no voltage was applied to the electrode, the electrode vibration had almost no effect on the value of $f_{\min}$ because there were no chains of particles. Figure 7 also shows that electrode vibration decreased f when the input voltage to the electrode was not zero.

Figure 8 shows some e–g relations measured under two extension rates without (Fig. 8a) and with (Fig. 8b) the electrode vibration. Figure 8a shows that the effect of the extension rate was small when the electrode vibration was not excited, suggesting that the value of c of the damper was small. However, Fig. 8b shows that the effect of the extension rate was large when the electrode vibration was excited, suggesting that the value of c was large.

The values of f and c were estimated by applying Eq. (1) of Ref. 6 to the d–p relations measured at two different extension/contraction rates. The estimated values of f and c are shown in Fig. 9 as functions of input voltage. Note that, just after the input voltage was turned off, the value of f at $V = 0$ was 1.0–1.1 N, more than twice the value shown in Fig. 9. Figure 9 shows that the value of f increased as the input voltage increased regardless of whether the electrode was vibrated. It also shows that, as suggested in Fig. 7, the electrode vibration decreased the value of f. Without electrode

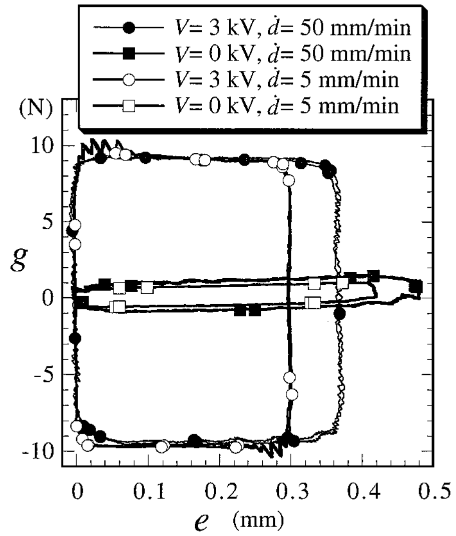

Fig. 8a Load-extension relations measured at two extension/contraction rates without electrode vibration.

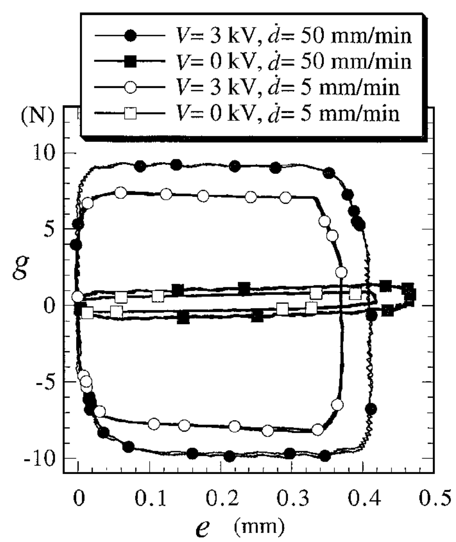

Fig. 8b Load-extension relations measured at two extension/contraction rates with electrode vibration.

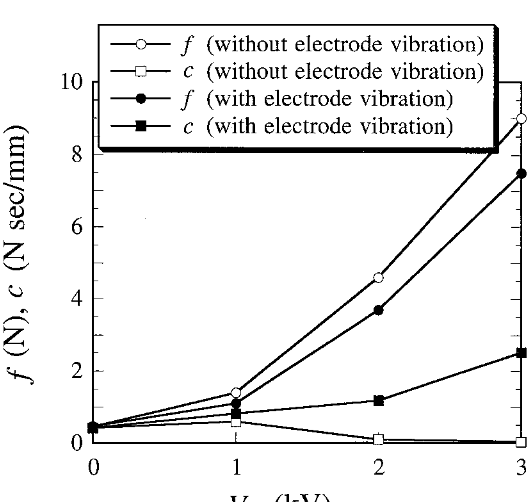

Fig. 9 Estimated values of f and c as functions of input voltage V with and without electrode vibration.

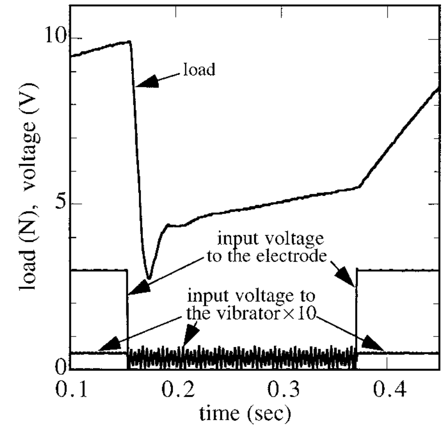

Fig. 10 Response of load on the damper to switching of the input voltage off and on during a constant-rate (20 mm/s) extension; input voltage to the vibrator modulated by a 1-kHz sampling frequency.

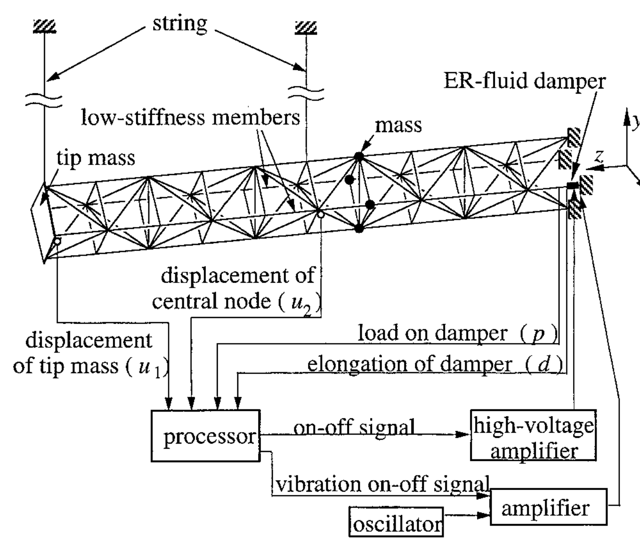

Fig. 11 Cantilevered 10-bay truss with an ER-fluid damper and block diagram of semiactive vibration-suppression experiment. (Masses at the four central nodes, the two low-stiffness members, and the u_2 sensor were for multiple-mode vibration suppression only.)

vibration, the value of c decreased with increasing voltage. With electrode vibration, however, the value of c increased, and this increase was especially obvious when the input voltage was more than 2 kV.

Figure 10 shows a time history of the load on the damper responding to the switching off and on of the input voltage during extension of the damper at a constant rate. The electrode vibration was excited only when the input voltage was turned off. In Fig. 10, the input voltage to the vibrator has been modulated by a sampling frequency. Figure 10 shows that the ER-fluid damper responds quickly, within a few milliseconds. The overshoot at the turning off of the input seems to be due to local dynamics of the damper or the experiment setup.

Semiactive Vibration Suppression Experiment

To see if the high-frequency vibration of the electrode is actually effective for semiactive vibration suppression, we performed experiments in which the LQFC-1-b on–off control law of Ref. 6 was applied to the same truss used in the work reported in Ref. 6. The experiment setup (Fig. 11) was the same as that used in Ref. 6 except that the oscillator, amplifier, and on–off signal line to the amplifier were added for excitation of the electrode vibration. The sensors for the measurements of displacements, load, and elongation were also the same as in Ref. 6. To investigate clearly the effectiveness of the electrode vibration, both single-mode and multiple-mode vibration suppression experiments were performed.

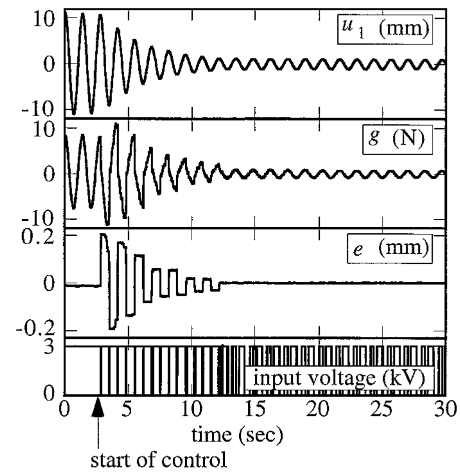

Fig. 12 Example time histories of semiactive suppression of single-mode vibration without electrode vibration.

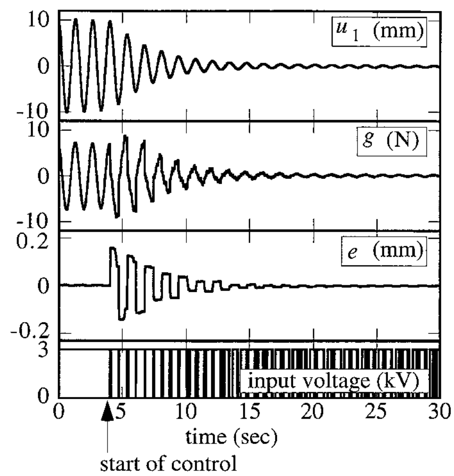

Fig. 13 Example time histories of semiactive suppression of single-mode vibration with electrode vibration.

Single-Mode Vibration Suppression Experiment

In the single-mode experiment, we tried to control only the first mode semiactively. For simplicity, the tip-mass displacement u_1 was assumed to be proportional to the first modal displacement. Under this assumption, e_T defined by Eq. (14) of Ref. 6 is proportional to $F_1 u_1 + F_2 \dot{u}_1$. Therefore, the control law Eq. (18) of Ref. 6 was implemented in terms of the measurable variables as follows because f was a monotonically increasing function of the input voltage V to the electrode:

$$V = 0 \quad \text{when} \quad \{(1 + k_2/k_1)p - k_2 d\}(F_1 u_1 + F_2 \dot{u}_1) \geq 0$$
$$V = V_{\max} \quad \text{when} \quad \{(1 + k_2/k_1)p - k_2 d\}(F_1 u_1 + F_2 \dot{u}_1) < 0 \tag{3}$$

The parameter values such as the weighting matrices for the linear quadratic regulator controller design were the same as those used in Ref. 6. In this experiment, $V_{\max}$ was 3 kV.

In the experiment, the tip mass was first displaced in the x direction by a certain amount, and then it was freed. Subsequently, the semiactive control Eq. (3) was started during the free vibration of the truss without exciting the electrode vibration. Figure 12 shows an example of the time histories thus obtained.

Figure 12 shows that when the vibration amplitude was large, e varied stepwise and dissipated energy effectively every time the input voltage was turned off. As a result, the vibration was suppressed rapidly. However, Fig. 12 shows that e ceased to respond to the turning off the input voltage at 13 s when the vibration was suppressed to a small amplitude, and the damper ceased to dissipate the energy. As a result, vibration almost ceased to damp. This was because the vibration was suppressed to so small an amplitude that the absolute value of g did not exceed $f_{\min}$ and the frictional element in Fig. 2 stuck even when the input voltage was turned off.

Next, the same experiment was performed with a 1.7-kHz electrode vibration. The electrode was vibrated only when the input voltage to the electrode was 0 kV. Figure 13 shows an example of the time histories thus obtained. Comparison of Figs. 13 and 12 reveals that both show similar suppression of large-amplitude vibration but show different degrees of suppression when the vibration amplitude is small. Figure 14, which compares some of the time histories in Fig. 13 with the corresponding histories in Fig. 12, shows that the vibration was suppressed to a much lower level when the electrode vibration was used. Without the electrode vibration, the amplitude of u_1 at 25 s was four times what it was with the electrode vibration. It can be seen in Figs. 12 and 14 that, without the electrode vibration, e did not vary even when g was approximately 1.0 N and V was zero, suggesting that the value of $f_{\min}$ was approximately 1.0 N. This value coincided with the value estimated from the measured flow friction in the bottleneck. With the electrode vibration, in contrast, e continued to vary for more than 20 s, dissipating the energy. The time histories of e and g of Figs. 13 and 14 indicate that, with the electrode vibration, e varied even when the absolute value of g was

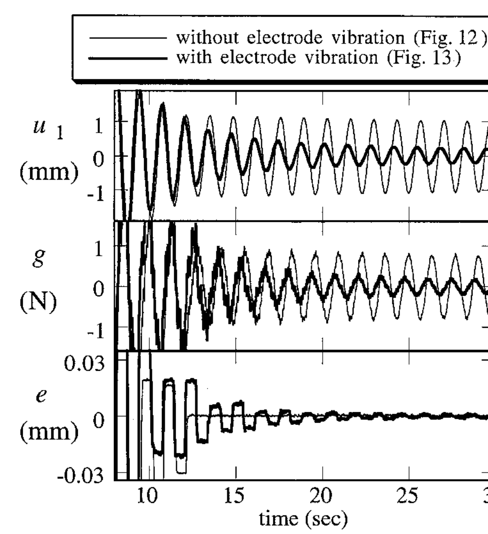

Fig. 14 Comparison of u_1, g, and e time histories in Figs. 12 and 13.

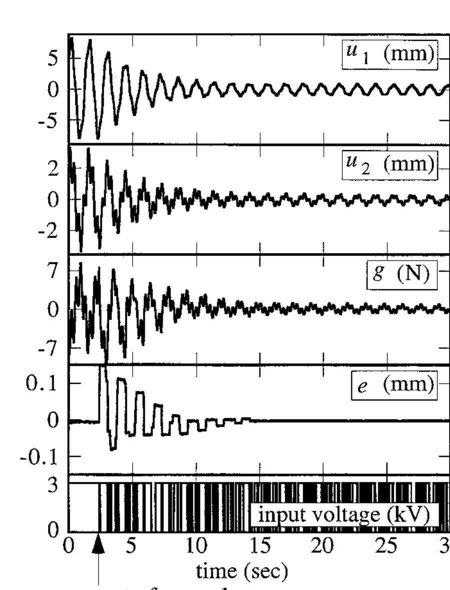

Fig. 15 Example time histories of semiactive suppression of two-mode vibration without electrode vibration.

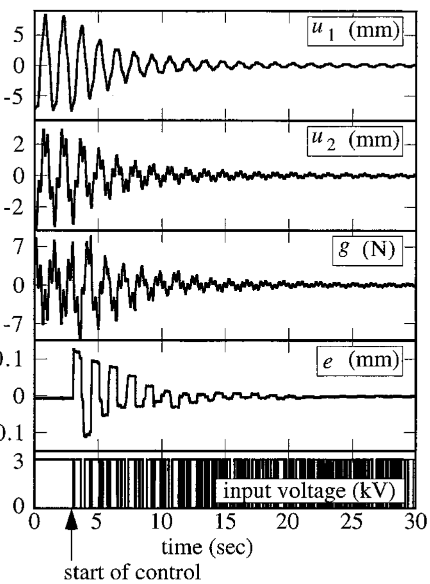

Fig. 16 Example time histories of semiactive suppression of two-mode vibration with electrode vibration.

as small as 0.3 N, suggesting that $f_{\min}$ was reduced to approximately 0.3 N by the electrode vibration in the actual dynamic condition.

Multiple-Mode Vibration Suppression Experiment

After the lowest two vibration modes in the x–z plane were excited by using a permanent magnet and a voice coil, the subsequent free vibrations of the two modes were suppressed semi-actively by using the LQFC-1-b control law implemented as Eq. (39) of Ref. 6. Example time histories obtained without the electrode vibration are shown in Fig. 15. Both the first and second modes damped quickly when the vibration amplitude was relatively large. As in Fig. 12, however, e did not vary after 15 s, and after the vibrations had been suppressed to small amplitudes they persisted. The time histories of e and g of Fig. 15 suggested that $f_{\min}$ was approximately 1.1 N during the persistent low-amplitude vibration.

The time histories shown in Fig. 16 were obtained in a similar experiment but with electrode vibration. Figure 16 shows the electrode vibration resulted in the amplitudes of vibration being suppressed to $\frac{2}{7}$ (at tip) and $\frac{2}{5}$ (at middle point) of what they were without the electrode vibration. The time histories of e and g of Fig. 16 suggests that $f_{\min}$ was approximately 0.5 N, less than half of what it was without the electrode vibration.

Conclusions

To improve performance of the ER-fluid damper for semiactive vibration suppression, a method to reduce the value of $f_{\min}$, especially the value just after turning off the high voltage to the electrode, by exploiting a high-frequency vibration of the electrode has been proposed and investigated.

The effect of the electrode vibration on $f_{\min}$ was first studied by measuring, with and without the electrode vibration, the flow friction in the bottleneck of the damper just after turning off the voltage to the electrode. The results clearly demonstrated a substantial effect of the electrode vibration on the flow friction, suggesting that the value of $f_{\min}$ just after turning off the voltage to the electrode can be reduced substantially by the electrode vibration. Because $f_{\max}$ can be kept unaffected by exciting the electrode vibration only when the input voltage to the electrode is turned off, the results suggested that the electrode vibration can substantially improve $f_{\max}/f_{\min}$, a performance index of the variable damper.

The effects of the electrode vibration on the characteristics of the damper were then investigated in extension/contraction tests with a constant input voltage to the electrode, the results of which showed that the electrode vibration decreases the value of f and increases the value of c when the input voltage is relatively high but has almost negligible effects when the input voltage is zero. The results of the flow friction measurement and the extension/contraction tests suggested that the electrode vibration reduces only the relatively large value of $f_{\min}$ just after turning off the input voltage.

Finally, the effect of the electrode vibration was investigated in experiments in which an ER-fluid damper was used for semiactive suppression of the vibration of a truss structure. Experiment results showed that the electrode vibration reduced the amplitudes of the truss vibrations to $\frac{1}{4}$–$\frac{2}{5}$ of what they were when the damper was used without electrode vibration. Investigation of the experiment results indicated that $f_{\min}$ in the dynamic condition of semiactive vibration suppression was reduced by factor of $\frac{1}{3}$–$\frac{1}{2}$ by the electrode vibration.

There are other approaches to increasing the value of $f_{\max}/f_{\min}$, for example, by improving the ER fluid, and the approach reported can be combined with other approaches to further increase the value of $f_{\max}/f_{\min}$.

References

[1] Onoda, J., Endo, T., Tamaoki, H., and Watanabe, N., "Vibration Suppression by Variable-Stiffness Members," *AIAA Journal*, Vol. 29, No. 6, 1991, pp. 977–983.

[2] Onoda, J., and Minesugi, K., "Semiactive Vibration Suppression of Truss Structures by Coulomb Friction," *Journal of Spacecraft and Rockets*, Vol. 31, No. 1, 1994, pp. 67–74.

[3] Wang, K. W., Kim, Y. S., and Shea, D. B., "Structural Vibration Control Via Electro-Rheological-Fluid-Based Actuators with Adaptive Viscous and Frictional Damping," *Journal of Sound and Vibration*, Vol. 177, No. 2, 1994, pp. 227–237.

[4] Choi, S.-B., and Park, Y.-K., "Active Vibration Control of a Cantilevered Beam Containing an Electro-Rheological Fluid," *Journal of Sound and Vibration*, Vol. 172, No. 3, 1994, pp. 428–432.

[5] Onoda, J., and Minesugi, K., "Semiactive Vibration Suppression by Variable-Damping Members," *AIAA Journal*, Vol. 34, No. 2, 1996, pp. 355–361.

[6] Onoda, J., Oh, H. U., and Minesugi, K., "Semiactive Vibration Suppression with Electrorheological-Fluid Dampers," *AIAA Journal*, Vol. 35, No. 12, 1997, pp. 1844–1852.

A. Berman
Associate Editor